Am J Transl Res 2026;18(6):5015-5027
www.ajtr.org /ISSN:1943-8141/AJTR0172358

Original Article

hsa_circ_0021001 modulates human brain vascular smooth muscle cell viability in intracranial aneurysm through the miR-152-3p/GREM1 axis

Jie Cao, Qiujiang Xi, Jianqing Yuan, Nanhai Liu, Haoquan Fan, Xiang Cao, Mingwei Guo

Department of Neurology, The First Affiliated Hospital of Gannan Medical University, Ganzhou 341000, Jiangxi, China

Received March 1, 2026; Accepted May 18, 2026; Epub June 15, 2026; Published June 30, 2026

Abstract: hsa_circ_0021001 is downregulated in intracranial aneurysm (IA), and this downregulation influences the growth of human brain vascular smooth muscle cells (hBVSMCs). However, the mechanism by which hsa_circ_0021001 contributes to hBVSMC dysfunction in IA remains unclear. In this study, the expressions of miR-152-3p, hsa_circ_0021001, and Gremlin 1 (GREM1) were detected using qRT-PCR. Cell viability was assessed using CCK-8 assays, protein levels of GREM1 and proliferating cell nuclear antigen (PCNA) were evaluated using western blotting. In addition, RNA immunoprecipitation (RIP) and dual-luciferase reporter assays were performed to validate the correlation among hsa_circ_0021001, GREM1, and miR-152-3p. Our results indicated that overexpression of hsa_circ_0021001 or GREM1 inhibited hBVSMC viability and migration, promoted cell apoptosis, decreased PCNA levels, and increased α-SMA levels. Additionally, miR-152-3p was shown to directly bind to both GREM1 and hsa_circ_0021001, reversing the effects of hsa_circ_0021001 on PCNA and α-SMA expression, hBVSMC viability, cell migration, and apoptosis. Inhibition of miR-152-3p suppressed hBVSMC viability and migration and promoted apoptosis, while GREM1 knockdwon rescued these cellular phenotypesthe and restored PCNA and α-SMA expression. In conclusion, hsa_circ_0021001 modulates GREM1 expression *via* miR-152-3p in hBVSMCs, thereby regulating IA-associated phenotypic alterations by suppressing cell viability and migration. It also promotes apoptosis through the miR-152-3p/GREM1 axis.

Keywords: hsa_circ_0021001, GREM1, intracranial aneurysm, miR-152-3p, vascular smooth muscle cells

Introduction

Intracranial aneurysms (IAs) are characterized by aberrant dilation of cerebral arteries, and rupture of an IA can lead to fatal subarachnoid hemorrhage [1]. Although the precise mechanisms underlying IA formation remain incompletely elucidated, alterations in the extracellular matrix of the vascular wall and dysfunction of vascular smooth muscle cells (VSMCs) have been implicated in its pathogenesis [2]. Particularly, phenotypic VSMC alterations, including enhanced proliferation and migration, are considered key contributors to IA pathogenesis [3]. However, the specific molecular pathways mediating these phenotypic alterations remain elusive.

Previous studies have demonstrated that IA pathophysiology involves complex interactions among various cellular components and molecular pathways within the arterial wall [4, 5]. Among these, the phenotypic transition of VSMCs from a contractile to a synthetic phenotype represents a key event in IA progression [6]. Aneurysm formation is associated with degeneration of the medial layer due to VSMC dissociation, migration from the media to intima, and enhanced proliferation [7]. Therefore, investigating VSMC proliferation and migration is of great significance for understanding IA pathogenesis. Assessing these functional alterations provides a more comprehensive understanding of VSMC phenotypic transition and their role in IA development, aligning with current perspectives on vascular remodeling.

Circular RNAs (circRNAs) are a class of non-coding RNAs characterized by a closed loop structure [8-10]. These RNAs can originate from

https://doi.org/10.62347/VHZH9735

exons, introns, or intergenic eukaryotic regions and exhibit tissue-specific expression pattern [11, 12]. Furthermore, circRNAs have been reported to play critical roles in IA progression [13-15]. For instance, circGNAQ regulates VSMC phenotypes and promotes apoptosis in IA [16]; hsa_circ_0008433 modulates VSMC function in IA pathogenesis [17]; and circ_0008571 regulates VSMCs' phenotype through miR-145-5p in IA [18].

hsa_circ_0021001 has been detected in peripheral blood and proposed as an IA biomarker [19]. However, its molecular mechanism in IA remains unclear although previous studies have shown that circRNA is lowly expressed in IA, and its biological function was validated by knocking down [20]. Additionally, because the hsa_circ_0021001 in this study is lowly expressed in IA, we validated its biological function by overexpressing hsa_circ_0021001.

The aim of this study was to investigate the downstream targets of hsa_circ_0021001 in IA and elucidate its role in regulating human brain VSMC (hBVSMC) phenotype. This work may provide novel insight into the pathogenesis of IA and identify therapeutic targets.

Materials and methods

Cell culture

Human 293T cells were obtained from American Type Culture Collection, or ATCC. hBVSMCs were obtained from Creative Bioarray and derived from human cerebral arteries. All cells were cultured in DMEM supplemented with glutamine, 10% FBS, and penicillin/streptomycin, and maintained in a humidified atmosphere with 5% CO_2 at 37°C.

Cell transfection

hBVSMCs were transfected with 50 nM miR-152-3p mimic, si-GREM1, or miR-152-3p inhibitor using Lipofectamine 2000 (Invitrogen, USA) according to the manufacturer's protocol. To overexpress hsa_circ_0021001 in hBVSMCs, cells were transfected with 1 μg of hsa_circ_0021001 plasmid or a control vector (Guangzhou Geneseed Biotech Co., Ltd.). After 2 days of transfection, cells were used for subsequent assays. The sequences were as follows: si-GREM1: 5'AAAUCGAUGGAUAUGCAACGA3'; si-NC: 5'UUCUCCGAACGUGUCACGU TT3'. The forward Alu sequence: 5' ctccacctcccaggttcaagcgattctcctccctcagcctcccgagtagctgggaccacaggcatgcaccaccatccccagctaatttttgcattattagtagagttgggatttcttcaccgtgttggccaggccggtcttggactcctgacctcaagtgatccaactgcctcagcctctcaaagtgctaggattacagggatctatacttttctgatattataaagatagttatcttctccaagggaaaaaatcatcttcatggaaattaatttacttttttacaaattgtgaatttgacccttaagagttttcttcctgatatttaaaattgaaaaaaaaattgttgacattaatatttcttctttc3', and backward Alu sequence: 5' tagctaacaactccatacttttttggttgtttattaatgtgaaatttctgctaaatgaaatacttttgtgtgtgtttgtggtagaagagaccacttcagttaaataaggaaatcaagagaggatcaatttaggaagattcagatatacagccgggtgcagtggctcatgcctgtaatccctgcacttagggaggctgaggcgggtggatgacctgaggttaggagttcaagaccagcctggccaacatggcgaaaccccatctctactaaaaataacaaaaattagctgggtgtggtggtgggtgtctataatcccagcaacttgggaggctgaggcaggagaatcac3'.

Quantitative reverse transcription polymerase chain reaction (qRT-PCR)

Total RNA (10 ng) was reverse transcribed using the iScript cDNA Synthesis Kit (170-8891, Bio-Rad). Then, qRT-PCR was performed using the SYBR Green PCR Kit (204001, Qiagen) on a Bio-Rad cycler. Relative expression levels of GREM1, hsa_circ_0021001, and miR-152-3p were determined using the $2^{-\Delta\Delta CT}$ method, normalized to GAPDH (for mRNA/circRNA) or U6 (for miRNA). All experiments were performed in triplicate. Primer sequences are shown in **Table 1**.

Cell viability analysis

Cell proliferation was assessed using the CCK-8 assays (C0038, Beyotime, China). Briefly, 1×10^4 cells per well were seeded in a 96-well plate and incubated for 24 h. Cells were then treated with CCK-8 solution (10 μL) for 1 h, and absorbance was measured at 450 nm using a microplate reader.

Transwell assay

Cell migration was assessed using Transwell chambers according to previous experimental methods [21]. Briefly, cells were seeded into the upper chamber in serum-free medium, while the lower chamber contained medium supplemented with 20% FBS. After 24 h incu-

Table 1. Sequences of primers

name	primer sequence
hsa_circ_0021001 F	5'-GCAGACCCAGCATGCACTG-3'
hsa_circ_0021001 R	5'-GGATCTCCATTGTGGCTGCC-3'
miR-152-3p F	5'-TCGGCAGGTCAGTGCATGACAGAA-3'
miR-152-3p R	5'-CTCAACTGGTGTCGTGGA-3'
GREM1 F	5'-GAGTTGCCTTGAGAGGGTCC-3'
GREM1 R	5'-TACTCGGGGATCGGCAAATG-3'
GAPDH F	5'-TGACGTGCCGCCTGGAGAAAC-3'
GAPDH R	5'-CCGGCATCGAAGGTGGAAGAG-3'
U6 F	5'-GAGGGCCTATTTCCCATGATT-3'
U6 R	5'-TAATTAGAATTAATTTGACT-3'

bation, migrated cells were fixed, stained with crystal violet, and photographed.

Cell apoptosis

Cell apoptosis was detected using flow cytometry (40302ES, Yeasen) according to the manufacturer's instructions. Cells were stained with Annexin V-FITC and PI, and apoptosis was quantified by flow cytometry.

Dual-luciferase reporter (DLR) assay

The 3'-UTR of GREM1 and hsa_circ_0021001 containing the predicted miR-152-3p binding regions were cloned into the pMIR-REPORT vector (Fubio). Cells were co-transfected with pRL-TK plasmid (50 ng), miRNA mimic (20 nM), and the indicated reporter plasmid (200 ng) for 24 h. Luciferase activity was measured using a dual-luciferase reporter assay system, and Renilla luciferase activity was used for normalization.

RNA immunoprecipitation (RIP) assay

RIP assays were performed to verify interactions between miR-152-3p and hsa_circ_0021001. Briefly, cells transfected with miR-152-3p mimics were lysed and incubated with anti-Argonaute-2 antibody (ab32381, Abcam, UK) or control IgG (ab172730, Abcam, UK) and Protein A/G magnetic beads. After centrifugation, the immunoprecipitated RNA was extracted, and enrichment of miR-152-3p and hsa_circ_0021001 was determined using qRT-PCR.

Western blotting

Total protein was extracted from cells or tissues using RIPA buffer with protease inhibitors. Proteins were separated by SDS-PAGE and transferred onto nitrocellulose membrane (Amersham, UK), which was then probed with primary antibodies against PCNA (1:1000), GREM1 (1:5000), and GAPDH (1:10000). After washing, membranes were incubated with HRP-labelled secondary anti-rabbit IgG antibody (1:1000, #7074, CST, USA) for 1 h and visualized using an enhanced chemiluminescence kit (#6883, CST). GAPDH served as an internal control.

Statistical analysis

Data were analyzed using GraphPad Prism 8.0 and were presented as means ± standard error (SE) or geometric mean with 95% confidence intervals (CIs). Comparisons between two two groups were performed using Student's t-test, and among multiple groups using one-way ANOVA followed by Tukey's post-hoc test. Repeated-measures ANOVA was applied for time-course data such as CCK-8 assays. A p-value < *0.05* was considered statistically significant.

Results

Effects of hsa_circ_0021001 on hBVSMC viability and migration

To investigate the stability and localization of hsa_circ_0021001, hBVSMC RNA was treated with RNase R. The results showed that hsa_circ_0021001 was resistant to RNase R-mediated degradation, while the corresponding linear transcript was markedly digested (**Figure 1A**). Furthermore, reverse transcription using random and oligo$(dT)_{18}$ primers revealed that hsa_circ_0021001 levels were reduced compared to those of the linear transcript when oligo$(dT)_{18}$ primers were used (**Figure 1B**), consistent with its circular nature. Moreover, the actinomycin D assay demonstrated that hsa_circ_0021001 had a longer half-life than the linear RNA (**Figure 1C**), suggesting high cellular stability. Subcellular fractionation assay indicated that hsa_circ_0021001 was substantially enriched in the cytoplasm of hBVSMCs (**Figure 1D**). Collectively, these data indicate that hsa_circ_0021001 is a circular, abundant, and stable transcript in IA.

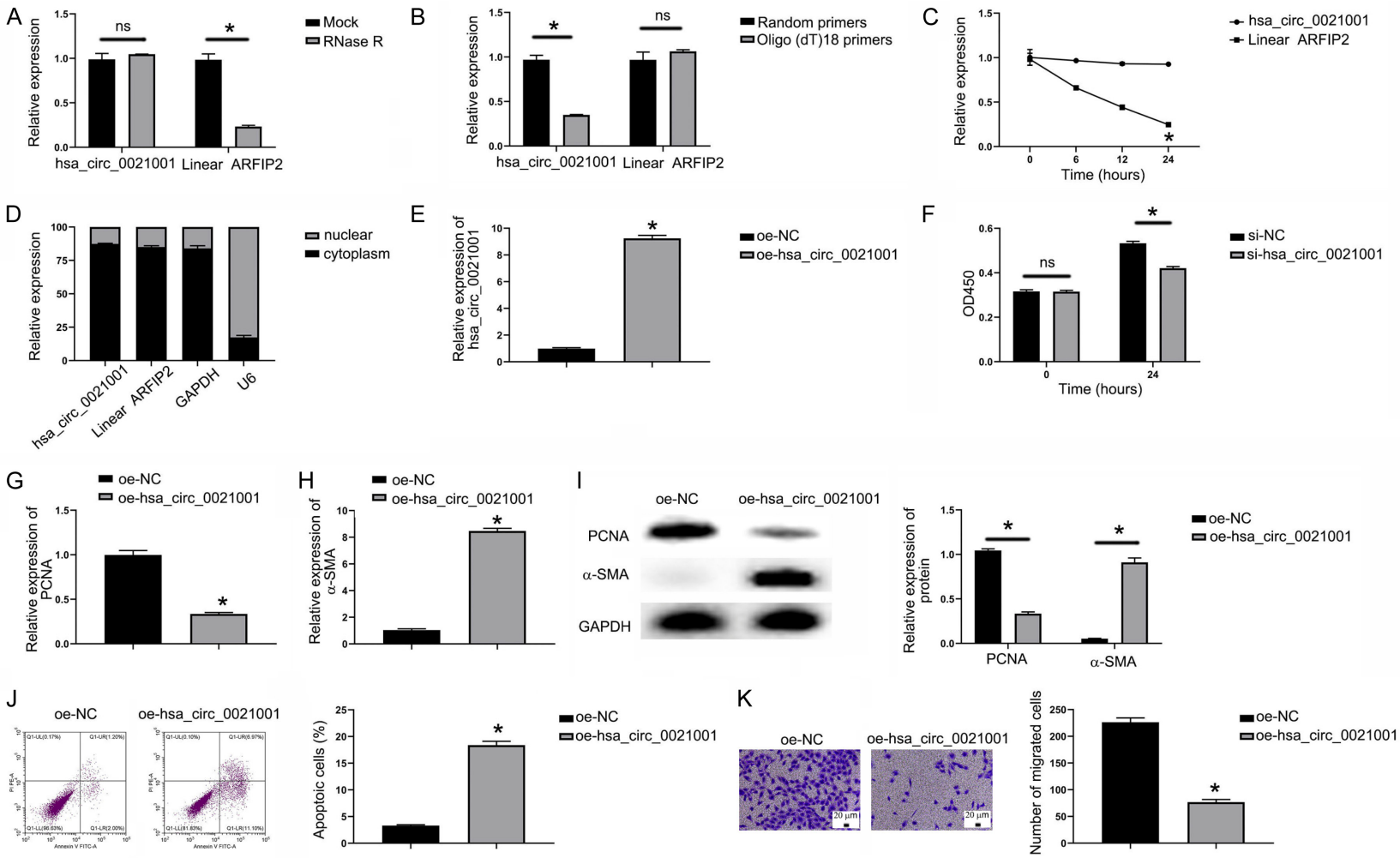

Figure 1. Effects of hsa_circ_0021001 on hBVSMC viability. A. RNase R assay showing the resistance of hsa_circ_0021001 to exonuclease digestion in hBVSMCs. B. qRT-PCR analysis of hsa_circ_0021001 and linear ARFIP2 mRNA expression using random and oligo(dT)18 primers in hBVSMCs. C. qRT-PCR analysis of circ_0021001 and linear ARFIP2 mRNA after treatment with Actinomycin D in hBVSMCs. D. Subcellular localization of hsa_circ_0021001 in nuclear and cytoplasmic fractions of hBVSMC. E. qRT-PCR analysis of hsa_circ_0021001 expression after transfection. F. hBVSMC viability was assessed using the CCK-8 assay. G-I. qRT-PCR and western blot analyses of PCNA and α-SMA levels in hBVSMCs. J. Flow cytometry analysis of cell apoptosis. K. Transwell assay detecting cell migration, with representative images captured at 200-fold magnification. *$P < 0.05$.

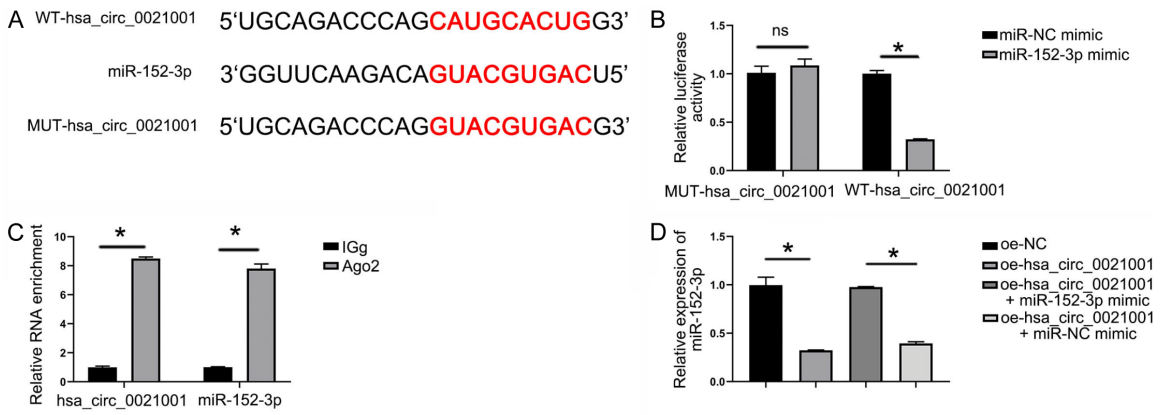

Figure 2. miR-152-3p is a target of hsa_circ_0021001. A. Schematics of the predicted binding sites between hsa_circ_0021001 and miR-152-3p. B. Dual-luciferase reporter assay in 293 T cells co-transfected with the reporter plasmid and miR-152-3p mimic or miRNA NC. C. RNA immunoprecipitation (RIP) assay showing enrichment of hsa_circ_0021001 and miR-152-3p in hBVSMCs using Anti-Ago2 or Anti-IgG antibodies. D. qRT-PCR analysis of miR-152-3p expression in hBVSMCs transfected with vector, hsa_circ_0021001, hsa_circ_0021001 + miR-NC, or hsa_circ_0021001 + miR-152-3p mimic. *$P < 0.05$.

To test the effect of hsa_circ_0021001 on hBVSMC viability, cells were transfected with a specific hsa_circ_0021001 overexpression plasmid, and qRT-PCR confirmed that hsa_circ_0021001 was markedly upregulated in hBVSMCs following transfection (**Figure 1E**). In addition, CCK-8 assays demonstrated that hBVSMC viability was substantially suppressed after hsa_circ_0021001 overexpression (**Figure 1F**). qPCR and western blot analyses revealed that PCNA levels were significantly decreased, while α-SMA levels were significantly elevated after hsa_circ_0021001 transfection (**Figure 1G-I**). Furthermore, hsa_circ_0021001 transfection significantly promoted cell apoptosis (**Figure 1J**) and suppressed cell migration (**Figure 1K**). Overall, these results indicate that hsa_circ_0021001 supresses hBVSMC viability and migration while promoting apoptosis.

miR-152-3p was identified as a target of hsa_circ_0021001

The StarBase website was employed to predict potential interaction between miR-152-3p and hsa_circ_0021001 (**Figure 2A**). DLR assay in 293T cells showed that co-transfection of both WT-hsa_circ_0021001 and miR-152-3p mimic substantially reduced luciferase activity compared to controls (**Figure 2B**). Moreover, RIP analysis revealed that both hsa_circ_0021001 and miR-152-3p were elevated in the Anti-Ago2 antibody compared to Anti-IgG antibody (**Figure 2C**). In addition, hsa_circ_0021001 overexpression in hBVSMCs decreased miR-152-3p levels, which were restored by co-transfection with the miR-152-3p mimic (**Figure 2D**). Collectively, these data suggest that hsa_circ_0021001 directly targets and suppresses miR-152-3p expression in hBVSMCs.

Hsa_circ_0021001 suppressed hBVSMC viability and migration by targeting miR-152-3p

To determine whether miR-152-3p mediates the effects of hsa_circ_0021001 on hBVSMCs, rescue experiments were performed. The results revealed that co-transfection with the miR-152-3p mimic reversed the inhibitory effects of hsa_circ_0021001 overexpression on hBVSMC viability (**Figure 3A**), counteracted the downregulation of PCNA and the upregulation of a-SMA induced by hsa_circ_0021001 (**Figure 3B-D**), and attenuated hsa_circ_0021001-induced apoptosis (**Figure 3E**). Additionally, miR-152-3p mimic attenuated hsa_circ_0021001-mediated suppression of hBVSMC migration (**Figure 3F**). These findings indicate that hsa_circ_0021001 modulates hBVSMCs viability, apoptosis, and migration by targeting miR-152-3p.

GREM1 was identified as a target of miR-152-3p

StarBase predictions identified potential binding sites between GREM1 and miR-152-3p

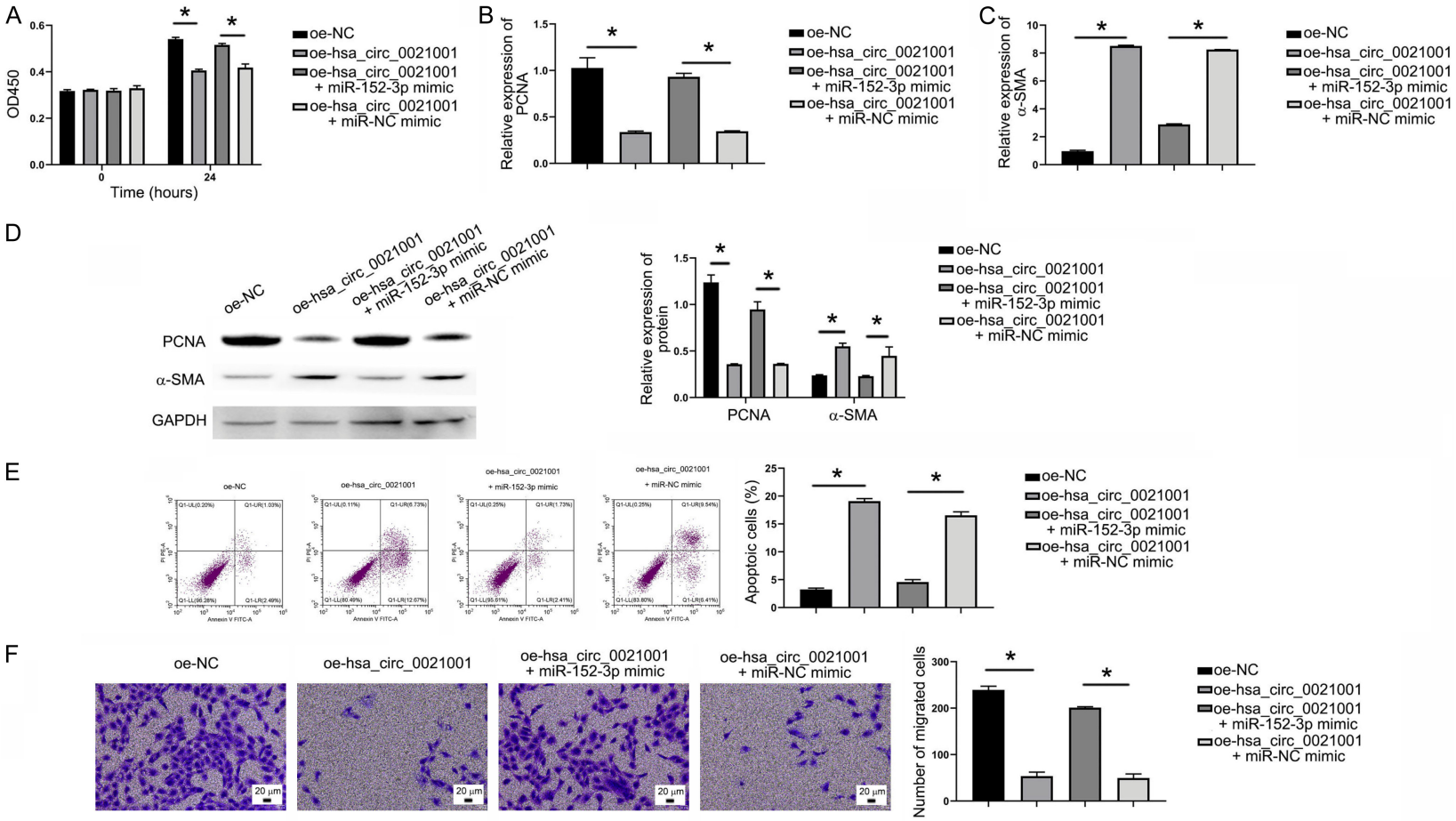

Figure 3. hsa_circ_0021001 regulated hBVSMC viability, apoptosis, and migration by targeting miR-152-3p. A. hBVSMC viability was evaluated by CCK-8 assay. B-D. qRT-PCR and western blot analyses of PCNA and α-SMA expression in hBVSMCs. E. Flow cytometric analysis of hBVSMC apoptosis. F. Transwell assay assessing hBVSMC migration, with representative images captured at 200-fold magnification. *$P < 0.05$.

(**Figure 4A**). Subsequent DLR assays demonstrated that the miR-152-3p mimic substantially decreased the luciferase activity of the wild-type GREM1 3' UTR reporter, rather than the mutant reporter (**Figure 4B**). Moreover, RIP assay confirmed that Anti-Ago2 antibody enriched both GREM1 and miR-152-3p compared to Anti-IgG antibody (**Figure 4C**), validating GREM1 as a miR-152-3p target in hBVSMCs. Functional assays showed that miR-152-3p mimic decreased GREM1 expression, while miR-152-3p inhibitor increased it. However, these effects were reversed by knockdown or overexpression, respectively (**Figure 4D-G**). Collectively, these data indicate that miR-152-3p targets GREM1 and negatively modulates its expression in hBVSMCs.

GREM1 reversed the effects of miR-152-3p on hBVSMC viability and migration

To investigate whether the miR-152-3p/GREM1 axis mediates hBVSMC dysfunction, hBVSMCs were co-transfected with miR-152-3p inhibitor and GREM1 siRNA. miR-152-3p inhibitor suppessed hBVSMCs viability, whereas GREM1 silencing reversed this effect (**Figure 5A**). Similarly, qPCR and western blot analyses revealed that GREM1 silencing mitigated miR-152-3p inhibitor-mediated decrease in PCNA and increases in α-SMA (**Figure 5B-D**). Additionally, GREM1 knockdown suppressed the miR-152-3p inhibitor-mediated increase in hBVSMC apoptosis (**Figure 5E**) and restored cell migration (**Figure 5F**). These findings indicate that miR-152-3p modulates hBVSMCs viability, apoptosis, and migration via GREM1.

Hsa_circ_0021001 indirectly modulated GREM1 through miR-152-3p in hBVSMCs

Given that hsa_circ_0021001 binds miR-152-3p and GREM1 is a target of miR-152-3p, we examined whether hsa_circ_0021001 indirectly regulates GREM1 through miR-152-3p. The results demonstrated that co-transfection of miR-152-3p mimic restored oe-hsa_circ_0021001-mediated GREM1 up-regulation both at protein and mRNA levels (**Figure 6A**, **6B**), indicating that hsa_circ_0021001 indirectly modulates GREM1 expression through miR-152-3p in hBVSMCs.

Discussion

Intracranial aneurysms are pathologic dilations of cerebral arteries caused by damage to the intracranial arterial wall. They represent a major cause of subarachnoid hemorrhage, and if ruptured, they result in severe complications or death [22, 23]. Studies indicate that the prevalence of IA is approximately 7.0% in individuals aged 35-75 years [24]. The pathogenesis of IA is complex and incompletely understood. Moreover, phenotypic modulation of VSMCs plays a critical role in IA development [16, 25-27]. *In vivo*, the dynamic balance between VSMC proliferation and apoptosis maintains development; however, disruption of this balance impairs VSMC function, reduces collagen fiber synthesis, and diminishes repair capacity, thus leading to IA formation [28]. Therefore, it is important to investigate the functional roles of hBVSMCs in IA for the development of effective therapeutic strategies.

Evidence indicates that circRNAs are key regulators in IA progression. For instance, circ_FOXO3 modulates KLF6 by sponging miR-122-5p, inhibiting H_2O_2-mediated hBVSMC proliferation, and thereby influencing IA progression in a cellular model [29]. Similarly, circRNA such as circLIFR regulate human VSMC proliferation, migration, invasion, and apoptosis *via* the miR-1299/KDR axis [30]. In addition, hsa_circ_0008433 has been found to regulate VSMC function in IA pathogenesis [17]. Notably, hsa_circ_0021001, identified in peripheral blood, has emerged as a novel biomarker for IA detection [19]. In the current study, hsa_circ_0021001 overexpression significantly suppressed hBVSMC viability and migration while promoting apoptosis, implying that hsa_circ_0021001 modulates VSMC phenotypic change. Addtionally, aneurysm formation involves degeneration of the arterial media due to VSMC dissociation, migration from the media to the intima, and increased proliferation [7]. Previous studies had reported that hsa_circ_0021001 is downregulated in IA patients [19]. Thus, downregulation of hsa_circ_0021001 in IA may promote hBVSMC phenotypic change, leading to increased hBVSMC migration and proliferation.

Previous studies suggested that circRNAs regulate gene expression by functioning as sponges for miRNAs [31-33]. Since hsa_circ_0021001 is predominantly localized to the cytoplasm of hBVSMCs, we hypothesized that it modulates hBVSMC viability by sponging miRNAs. Subsequent bioinformatic predictions identified miR-152-3p as a potential

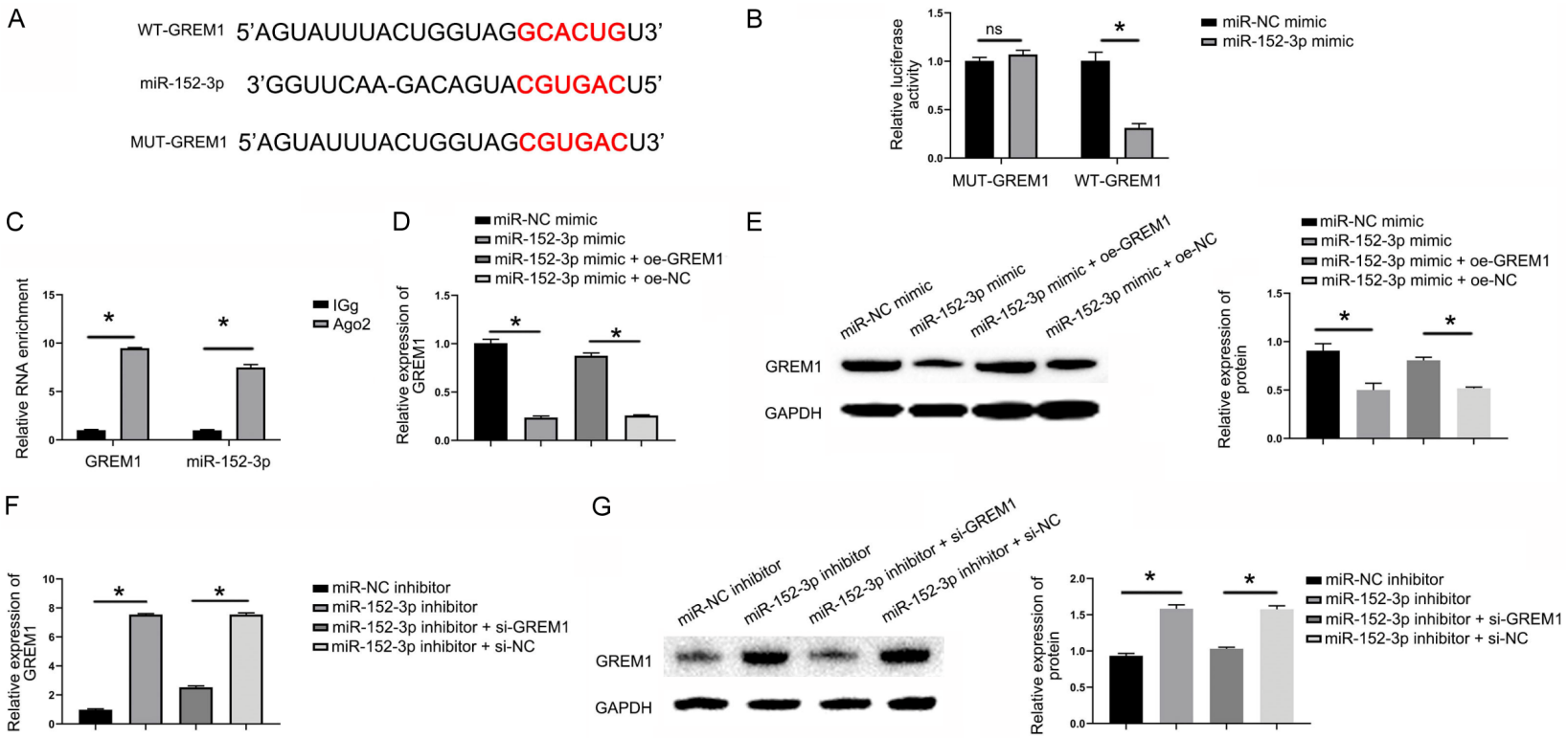

Figure 4. GREM1 is a target of miR-152-3p. A. Schematics of the predicted binding sites comparing GREM1 and miR-152-3p. B. Dual-luciferase reporter assay in 293 T cells co-transfected with the reporter plasmid and miR-152-3p mimic or miRNA NC. C. RNA immunoprecipitation (RIP) assay showing enrichment of GREM1 and miR-152-3p in hBVSMCs using Anti-Ago2 or Anti-IgG antibodies. D-G. qRT-PCR and western blot analyses of GREM1 expression in hBVSMCs under different treatment conditions. *$P < 0.05$.

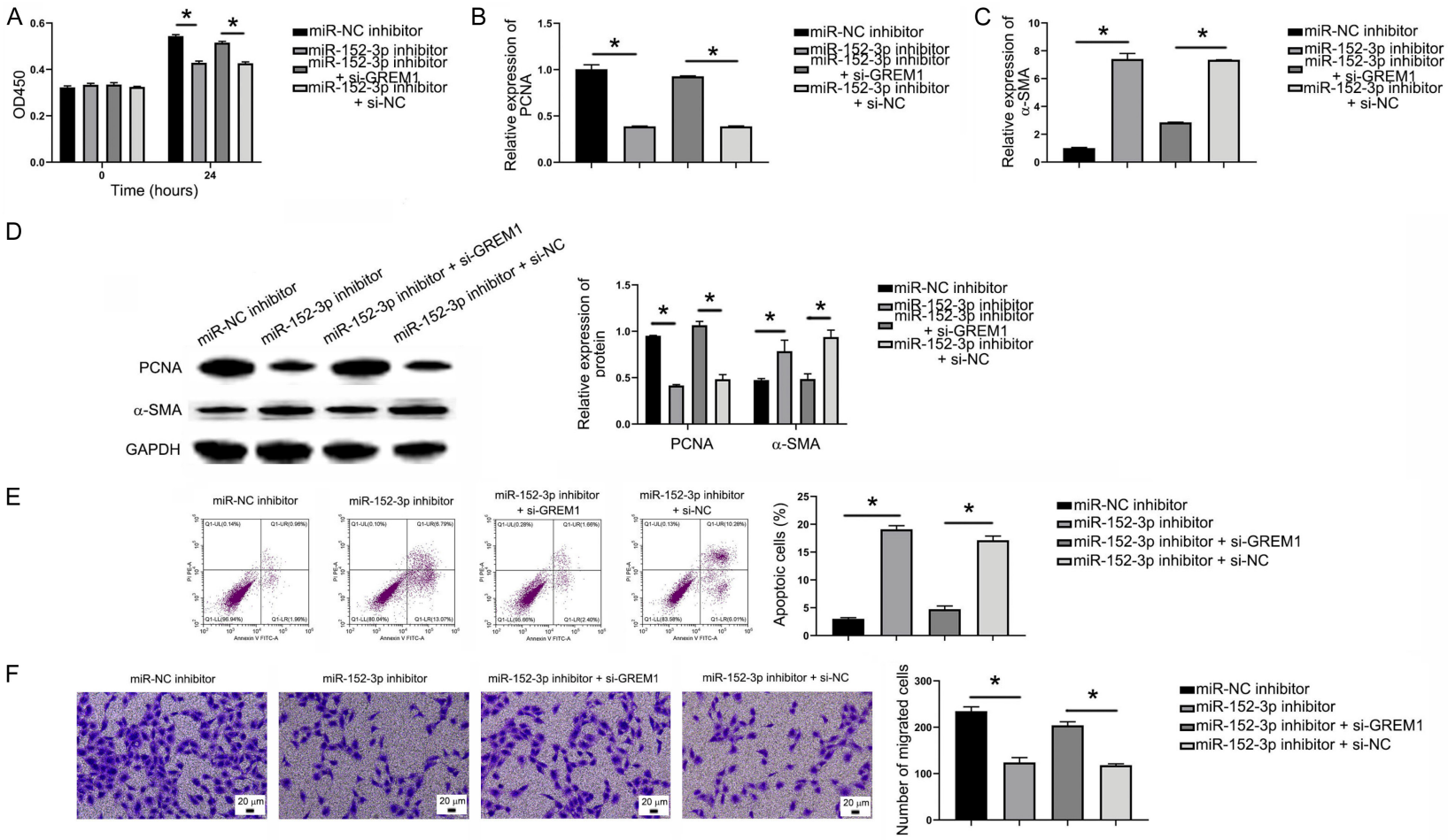

Figure 5. GREM1 reversed the effects of miR-152-3p on hBVSMC viability. A. hBVSMC viability was evaluated by CCK-8 assays. B-D. qRT-PCR and western blot analyses of PCNA expression in hBVSMCs. E. Flow cytometry analysis of cell apoptosis. F. Transwell assay assessing hBVSMC migration, with representative images captured at 200-fold magnification. *$P < 0.05$.

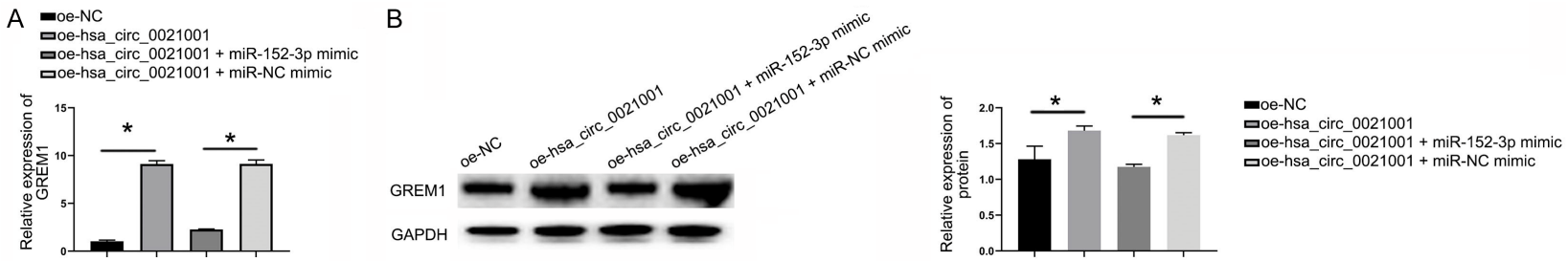

Figure 6. Hsa_circ_0021001 indirectly regulated GREM1 expression through miR-152-3p in hBVSMCs. A, B. qRT-PCR and western blot analysis of GREM1 expression in hBVSMCs transfected with oe-NC, oe-hsa_circ_0021001, oe-hsa_circ_0021001 + miR-NC inhibitor, or oe-hsa_circ_0021001 + miR-152-3p inhibitor. *$P < 0.05$.

target of hsa_circ_0021001. Co-transfection with the miR-152-3p mimic reversed hsa_circ_0021001-induced decrease in hBVSMC viability and migration, as well as the increase in apoptosis. Notably, although miR-152-3p has not been reported in hBVSMCs, it has been implicated in the regulation of proliferation and migration in various tumor cells. For example, miR-152-3p promotes cell adhesion and hepatic metastases in colorectal cancer [34], and facilitates cell proliferation in chronic myeloid leukemia by inhibiting p27 [35]. These findings suggest that miR-152-3p may generally promote cell proliferation and migration.

DLR assays further identified GREM1 as a direct target of miR-152-3p. hsa_circ_0021001 overexpression increased GREM1 expression, while miR-152-3p mimic had opposite effects. VSMCs exhibit phenotypeic plasticity, including contractile, proliferative, migratory, and synthetic states [36]. BMP-2 is known to promote VSMC proliferation and migration, facilitating the switch to a synthetic phenotype through cytoskeletal remodeling, CD44, and matrix metalloproteinase pathways [37, 38]. GREM1, as a BMP antagonist, binds to BMP-2, 4, and 7 and prevents their interaction with BMP receptors on the cell membrane [39]. Thus, it is plausible that GREM1 modulates hBVSMC phenotypic changes through suppressing the BMP signaling pathway, a mechanism supported by our findings. Collectively, hsa_circ_0021001 regulates hBVSMC phenotypic alterations in IA by adsorbing miR-152-3p and thereby upregulating GREM1.

This study has several limitations. First, the expression of hsa_circ_0021001 in clinical IA tissue samples was not detected in this study, although previous studies have reported relevant evidence. Second, the mechanistic investigation only focused on the circRNA/miRNA/mRNA regulatory axis of hsa_circ_0021001, without further exploration of other potential molecular pathways. These aspects represent important directions for future research. Nevertheless, the current findings still provide novel insight into the molecular mechanisms underlying IA development and the functional role of hBVSMCs in this process.

Conclusions

hsa_circ_0021001 suppresses phenotypic alterations of hBVSMCs *in vitro* by upregulating GREM1 through miR-152-3p sponging. These results demonstrate that the hsa_circ_0021001/miR-152-3p/GREM1 axis plays a critical role in modulating IA pathogenesis.

Disclosure of conflict of interest

None.

Address correspondence to: Mingwei Guo, Department of Neurology, The First Affiliated Hospital of Gannan Medical University, No. 128 Jinling Road, Zhanggong District, Ganzhou 341000, Jiangxi, China. Tel: +86-15083930426; E-mail: Xiaoguo113@126.com

References

[1] Brinjikji W, Zhu YQ, Lanzino G, Cloft HJ, Murad MH, Wang Z and Kallmes DF. Risk factors for growth of intracranial aneurysms: a systematic review and meta-analysis. AJNR Am J Neuroradiol 2016; 37: 615-620.

[2] Frösen J. Smooth muscle cells and the formation, degeneration, and rupture of saccular intracranial aneurysm wall--a review of current pathophysiological knowledge. Transl Stroke Res 2014; 5: 347-356.

[3] Starke RM, Chalouhi N, Ding D, Raper DM, McKisic MS, Owens GK, Hasan DM, Medel R and Dumont AS. Vascular smooth muscle cells in cerebral aneurysm pathogenesis. Transl Stroke Res 2014; 5: 338-346.

[4] Cannizzaro D, Zaed I, Olei S, Fernandes B, Peschillo S, Milani D and Cardia A. Growth and rupture of an intracranial aneurysm: the role of wall aneurysmal enhancement and CD68. Front Surg 2023; 10: 1228955.

[5] Morel S, Bijlenga P and Kwak BR. Intracranial aneurysm wall (in)stability-current state of knowledge and clinical perspectives. Neurosurg Rev 2022; 45: 1233-1253.

[6] He J, Duan Y, Jiang Y, Luo J, Wang T, Liang R and Tang T. Phosphorylated NPY1R regulates phenotypic transition of vascular smooth muscle cells, inflammatory response and macrophage infiltration to promote intracranial aneurysm progression. Neuropeptides 2024; 108: 102465.

[7] Chalouhi N, Ali MS, Jabbour PM, Tjoumakaris SI, Gonzalez LF, Rosenwasser RH, Koch WJ and Dumont AS. Biology of intracranial aneurysms: role of inflammation. J Cereb Blood Flow Metab 2012; 32: 1659-1676.

[8] Kristensen LS, Andersen MS, Stagsted LVW, Ebbesen KK, Hansen TB and Kjems J. The biogenesis, biology and characterization of circular RNAs. Nat Rev Genet 2019; 20: 675-691.

[9] Huang A, Zheng H, Wu Z, Chen M and Huang Y. Circular RNA-protein interactions: functions,

mechanisms, and identification. Theranostics 2020; 10: 3503-3517.
[10] Ebbesen KK, Kjems J and Hansen TB. Circular RNAs: Identification, biogenesis and function. Biochim Biophys Acta 2016; 1859: 163-168.
[11] Chen I, Chen CY and Chuang TJ. Biogenesis, identification, and function of exonic circular RNAs. Wiley Interdiscip Rev RNA 2015; 6: 563-579.
[12] Kulcheski FR, Christoff AP and Margis R. Circular RNAs are miRNA sponges and can be used as a new class of biomarker. J Biotechnol 2016; 238: 42-51.
[13] Huang Q, Huang QY, Sun Y and Wu S. High-throughput data reveals novel circular RNAs via competitive endogenous RNA networks associated with human intracranial aneurysms. Med Sci Monit 2019; 25: 4819-4830.
[14] Wang Y, Wang Y, Li Y, Wang B, Miao Z Liu X and Ma Y. Decreased expression of circ_0020397 in intracranial aneurysms may be contributing to decreased vascular smooth muscle cell proliferation via increased expression of miR-138 and subsequent decreased KDR expression. Cell Adh Migr 2019; 13: 220-228.
[15] Gareev I, Shumadalova A, Ilyasova T, Beilerli A and Shi H. Circular RNAs in intracranial aneurysms: emerging roles in pathogenesis, diagnosis and therapeutic intervention. Noncoding RNA Res 2023; 9: 211-220.
[16] Zhou H, Wang C, Wang W, Guo P, Xu Y, Cui Z, Li X, Li S, Feng Y and Yu T. CircGNAQ promotes intracranial aneurysm formation by facilitating vascular smooth muscle cell phenotypic switching and apoptosis. Antioxid Redox Signal 2026; 44: 24-40.
[17] Wang F, Huang QY, Zeng YL, Kang XD and Huang Q. Circular RNA hsa_circ_0008433 drives vascular smooth muscle cell modulation in intracranial aneurysm pathogenesis. Adv Clin Exp Med 2025; 34: 1701-1710.
[18] Lu Z, Zhu S, Wu Y, Xu X, Li S and Huang Q. Circ_0008571 modulates the phenotype of vascular smooth muscle cells by targeting miR-145-5p in intracranial aneurysms. Biochim Biophys Acta Mol Basis Dis 2024; 1870: 167278.
[19] Teng L, Chen Y, Chen H, He X, Wang J, Peng Y, Duan H, Li H, Lin D and Shao B. Circular RNA hsa_circ_0021001 in peripheral blood: a potential novel biomarker in the screening of intracranial aneurysm. Oncotarget 2017; 8: 107125-107133.
[20] Xu J and Fang C. Circ-ATL1 silencing reverses the activation effects of SIRT5 on smooth muscle cellular proliferation, migration and contractility in intracranial aneurysm by adsorbing miR-455. BMC Mol Cell Biol 2023; 24: 3.
[21] Gao G, Zhang Y, Chao Y, Niu C, Fu X and Wei J. miR-4735-3p regulates phenotypic modulation of vascular smooth muscle cells by targeting HIF-1-mediated autophagy in intracranial aneurysm. J Cell Biochem 2019; 120: 19432-19441.
[22] Bederson JB, Connolly ES Jr, Batjer HH, Dacey RG, Dion JE, Diringer MN, Duldner JE Jr, Harbaugh RE, Patel AB and Rosenwasser RH; American Heart Association. Guidelines for the management of aneurysmal subarachnoid hemorrhage: a statement for healthcare professionals from a special writing group of the Stroke Council, American Heart Association. Stroke 2009; 40: 994-1025.
[23] Hashimoto T, Meng H and Young WL. Intracranial aneurysms: links among inflammation, hemodynamics and vascular remodeling. Neurol Res 2006; 28: 372-380.
[24] Li MH, Chen SW, Li YD, Chen YC, Cheng YS, Hu DJ, Tan HQ, Wu Q, Wang W, Sun ZK, Wei XE, Zhang JY, Qiao RH, Zong WH, Zhang Y, Lou W, Chen ZY, Zhu Y, Peng DR, Ding SX, Xu XF, Hou XH and Jia WP. Prevalence of unruptured cerebral aneurysms in Chinese adults aged 35 to 75 years: a cross-sectional study. Ann Intern Med 2013; 159: 514-521.
[25] Li Z, Huang J, Yang L, Li X and Li W. WNTA5-mediated miR-374a-5p regulates vascular smooth muscle cell phenotype transformation and M1 macrophage polarization impacting intracranial aneurysm progression. Sci Rep 2024; 14: 559.
[26] Sun ZH, Liu F, Kong LL, Ji PM, Huang L, Zhou HM, Sun R, Luo J and Li WZ. Interruption of TRPC6-NFATC1 signaling inhibits NADPH oxidase 4 and VSMCs phenotypic switch in intracranial aneurysm. Biomed Pharmacother 2023; 161: 114480.
[27] Guo Z, Zhong Y, Ming Z and Wang Y. METTL3 promotes vascular stability in intracranial aneurysm via m6A-AMPK axis. Sci Rep 2025; 15: 41774.
[28] Kovacevic M, Jonjic N, Stalekar H, Zaputovic L, Stifter S and Vitezic D. Apoptotic cell death and rupture of abdominal aortic aneurysm. Med Hypotheses 2010; 74: 908-910.
[29] Yue PD, Lu YN, Zhang L and Ma ZF. Circ_FOXO3 regulates KLF6 through sponge adsorption of miR-122-5p to repress H2O2-induced HBVSMC proliferation, thus promoting IA development in vitro model. Acta Biochim Pol 2022; 69: 767-772.
[30] Zhang H, Zhang B, Chen C and Chen J. Circular RNA circLIFR regulates the proliferation, migration, invasion and apoptosis of human vascular smooth muscle cells via the miR-1299/KDR axis. Metab Brain Dis 2022; 37: 253-263.

[31] Liu X, Jiang L, Zeng H, Gao L, Guo S, Chen C, Liu X, Zhang M, Ma L, Li Y, Qi X and Wu Y. Circ-0000953 deficiency exacerbates podocyte injury and autophagy disorder by targeting Mir665-3p-Atg4b in diabetic nephropathy. Autophagy 2024; 20: 1072-1097.
[32] Yang X, Liu R, Du Y, Mei C, Zhang G, Wang C, Yang Y, Xu Z, Li W and Liu X. circRNA_8521 promotes Senecavirus A infection by sponging miRNA-324 to regulate LC3A. Vet Res 2024; 55: 43.
[33] Wu Y, Zheng Z, Bai X, Liu P, Hu S, Wang L and Yang S. CircRNA_0003307 promoted brain microvascular endothelial cell angiogenesis, invasion, and migration in cerebral ischemia-reperfusion injury: potential involvement of miRNA-191-5p/CDK6 pathway. Neuroscience 2024; 560: 77-89.
[34] Zhu X, Jin X, Li Z, Chen X and Zhao J. miR-152-3p facilitates cell adhesion and hepatic metastases in colorectal cancer via targeting AQP11. Pathol Res Pract 2023; 244: 154389.
[35] Wang L, Wang Y and Lin J. MiR-152-3p promotes the development of chronic myeloid leukemia by inhibiting p27. Eur Rev Med Pharmacol Sci 2018; 22: 8789-8796.
[36] Matchkov VV, Kudryavtseva O and Aalkjaer C. Intracellular Ca(2)(+) signalling and phenotype of vascular smooth muscle cells. Basic Clin Pharmacol Toxicol 2012; 110: 42-48.
[37] Yang M, Fan Z, Wang F, Tian ZH, Ma B, Dong B, Li Z, Zhang M and Zhao W. BMP-2 enhances the migration and proliferation of hypoxia-induced VSMCs via actin cytoskeleton, CD44 and matrix metalloproteinase linkage. Exp Cell Res 2018; 368: 248-257.
[38] Zhang X, Huang T, Zhai H, Peng W, Zhou Y, Li Q and Yang H. Inhibition of lysine-specific demethylase 1A suppresses neointimal hyperplasia by targeting bone morphogenetic protein 2 and mediating vascular smooth muscle cell phenotype. Cell Prolif 2020; 53: e12711.
[39] Topol LZ, Bardot B, Zhang Q, Resau J, Huillard E, Marx M, Calothy G and Blair DG. Biosynthesis, post-translation modification, and functional characterization of Drm/Gremlin. J Biol Chem 2000; 275: 8785-8793.